www.czasopisma.pan.pl PAN POLSKA AKADEMIA NAUK www.journals.pan.pl

ARCHIVES OF ACOUSTICS
Arch. Acoust., **35**, 1, 13–33 (2010)

DOI: 10.2478/v10168-010-0002-8

Optimization of Multi-Chamber Mufflers with Reverse-Flow Ducts by Algorithm of Simulated Annealing

Ying-Chun CHANG, Min-Chie CHIU

(1) *Tatung University*
Department of Mechanical Engineering
40 Chungshan N. Rd., Sec. 3, Taipei, 104, R.O.C.
e-mail: ycchang@ttu.edu.tw

(2) *ChungChou Institute of Technology*
Department of Automatic Control Engineering
6, Lane 2, Sec. 3, Shanchiao Rd., Yuanlin
Changhua 51003, Taiwan, R.O.C.
e-mail: minchie.chiu@msa.hinet.net

(*received June 24, 2009; accepted November 13, 2009*)

Shape optimization on mufflers within a limited space volume is essential for industry, where the equipment layout is occasionally tight and the available space for a muffler is limited for maintenance and operation purposes. To proficiently enhance the acoustical performance within a constrained space, the selection of an appropriate acoustical mechanism and optimizer becomes crucial. A multi-chamber side muffler hybridized with reverse-flow ducts which can visibly increase the acoustical performance is rarely addressed; therefore, the main purpose of this paper is to numerically analyze and maximize the acoustical performance of this muffler within a limited space.

In this paper, the four-pole system matrix for evaluating the acoustic performance – sound transmission loss (STL) – is derived by using a decoupled numerical method. Moreover, a simulated annealing (SA) algorithm, a robust scheme in searching for the global optimum by imitating the softening process of metal, has been used during the optimization process. Before dealing with a broadband noise, the *STL's* maximization with respect to a one-tone noise is introduced for the reliability check on the SA method. Moreover, the accuracy check of the mathematical models with respect to various acoustical elements is performed.

The optimal result in eliminating broadband noise reveals that the multi-chamber muffler with reverse-flow perforated ducts is excellent for noise reduction. Consequently, the approach used for the optimal design of the noise elimination proposed in this study is easy and effective.

Keywords: multi-chamber muffler, reverse-flow, decoupled numerical method, space constraints, simulated algorithm.

Notations

This paper is constructed on the basis of the following notations:

C_o – sound speed (m s^{-1}),
C – the Boltzmann constant,
dh_i – the diameter of a perforated hole on the i-th inner tube (m),
T – the current temperature (°C),
D – diameter of the tubes (m),
f – cyclic frequency (Hz),
$iter$ – maximum iteration,
j – imaginary unit,
k – wave number ($= \omega/c_o$),
kk – cooling rate in SA,
L_1, L_2 – lengths of inlet/outlet straight ducts (m),
L_0 – total length of the muffler (m),
M – mean flow Mach number,
OBJ_i – objective function (dB),
p – acoustic pressure (Pa),
$\overline{p}_i$ – acoustic pressure at the i-th node (Pa),
$pb(T)$ – transition probability,
Q – volume flow rate of venting gas ($m^3 s^{-1}$),
S_i – section area at the i-th node(m^2),
STL – sound transmission loss (dB),
$SWLO$ – unsilenced sound power level inside the muffler's inlet (dB),
SWL_T – overall sound power level inside the muffler's output (dB),
t_i – the thickness of the i-th inner perforated tube (m),
$TE1_{i,j}$, $TE2_{i,j}$ – components of four-pole transfer matrices for an acoustical mechanism with internal extended ducts,
$TS1_{i,j}$, $TS2_{i,j}$, $TS3_{i,j}$, $TS4_{i,j}$, $TS5_{i,j}$, $TS6_{i,j}$ – components of four-pole transfer matrices for an acoustical mechanism with straight ducts,
$TSE1_{i,j}$, $TSE2$ – components of four-pole transfer matrices for an acoustical mechanism with a side inlet/outlet,
$TPRF_{i,j}$ – components of a four-pole transfer matrix for an acoustical mechanism with reverse-flow perforated ducts,
T^*_{ij} – components of a four-pole transfer system matrix,
u – acoustic particle velocity (m s^{-1}),
$\overline{u}_i$ – acoustic particle velocity at the i-th node (m s^{-1}),
V_i – mean flow velocity at the i-th node (m s^{-1}),
ρ_o – air density (kg m^{-3}),
ρ_i – acoustical density at the i-th node,
η_i – the porosity of the i-th inner perforated tube.

1. Introduction

Because high noise levels induce psychological and physiological ailments (Alley *et al.*, 1989), the requirement of low-noise levels of various products has become crucial. To overcome the low-frequency noise emitted from a venting system, a muffler has been continually used (Magrab, 1975). The research of

mufflers was started by Davis *et al.* (1954). To increase a muffler's acoustical performance, the assessment of a new acoustical element – a reverse-flow mechanism with double internal perforated tubes – was proposed and investigated by Munjal *et al.* (1987). On the basis of coupled differential equations, a series of theories and numerical techniques in decoupling the acoustical problems have been proposed (Munjal *et al.*, 1987; Sullivan, Crocker, 1978; Sullivan, 1979a, 1979b; Thawani, Jayaraman, 1983). Considering the flowing effect, Munjal (1987), and Peat (1988) publicized the generalized decoupling and numerical decoupling methods, which overcome the drawbacks seen in the previous studies.

Because the constrained problem is mostly concerned with the necessity of operation and maintenance in the industry, there is a growing need to optimize the acoustical performance within a fixed space. Yet the need to investigate the optimal muffler design under space constraints is rarely tackled. In previous papers, the shape optimizations of simple-expansion mufflers were discussed (Yeh *et al.*, 2003; Chang *et al.*, 2004; 2005; Yeh *et al.*, 2006). In dealing with a venting noise emitted from the side, side inlet/outlet mufflers have been frequently used. To greatly increase the acoustical performance within a fixed space, a new acoustical mechanism of multi-chamber mufflers hybridized with reverse-flow perforated tubes arrived at by using the novel scheme of simulated annealing (*SA*) is presented.

In this paper, the *SA* method, a stochastic relaxation technique originated by Metropolis *et al.* (1953) and developed by Kirkpatrick *et al.* (1983) imitating the physical process of annealing metal to reach the minimum energy state, is applied in this work.

2. Theoretical background

In this paper, a multi-chamber side inlet/outlet muffler with reverse-flow perforated tubees was adopted for noise elimination in the air compressor room shown in Fig. 1. The outlines of these mufflers are shown in Fig. 2. Before the acoustical fields of mufflers are analyzed, the acoustical elements have to be distinguished. As shown in Fig. 3, four kinds of muffler components, including straight duct, side inlet/outlet duct, internally extended duct, and reverse-flow perforated duct, are identified and symbolized as I, II, III, and IV. In addition, the acoustic pressure $\overline{p}$ and acoustic particle velocity $\overline{u}$ within the muffler are depicted in Fig. 4, where the acoustical field is represented by seventeen nodes.

In previous study (Chiu, 2009), the general approach to apply the four-pole matrix system to evaluate the acoustic performance of mufflers has been applied to the case of multi-chamber mufflers hybridized with perforated plug-inlet under space constrains. In this paper, after applying similar approach and deriving adequate formulas, we present results for the case of optimization of multi-chamber mufflers with reverse-flow ducts by algorithm of simulated annealing.

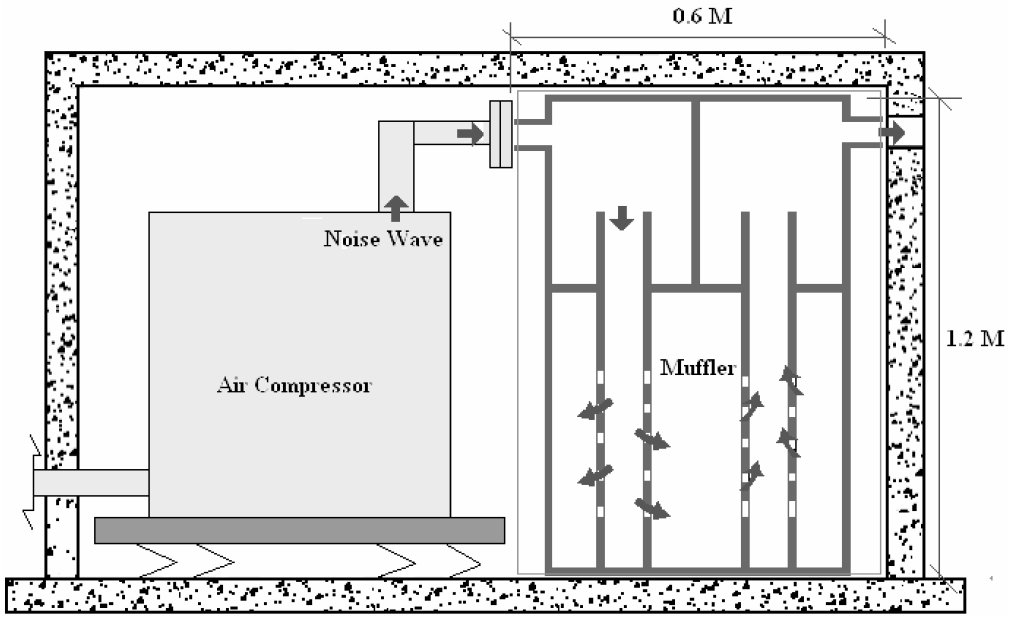

Fig. 1. Noise elimination of an air-compressor noise inside a limited space.

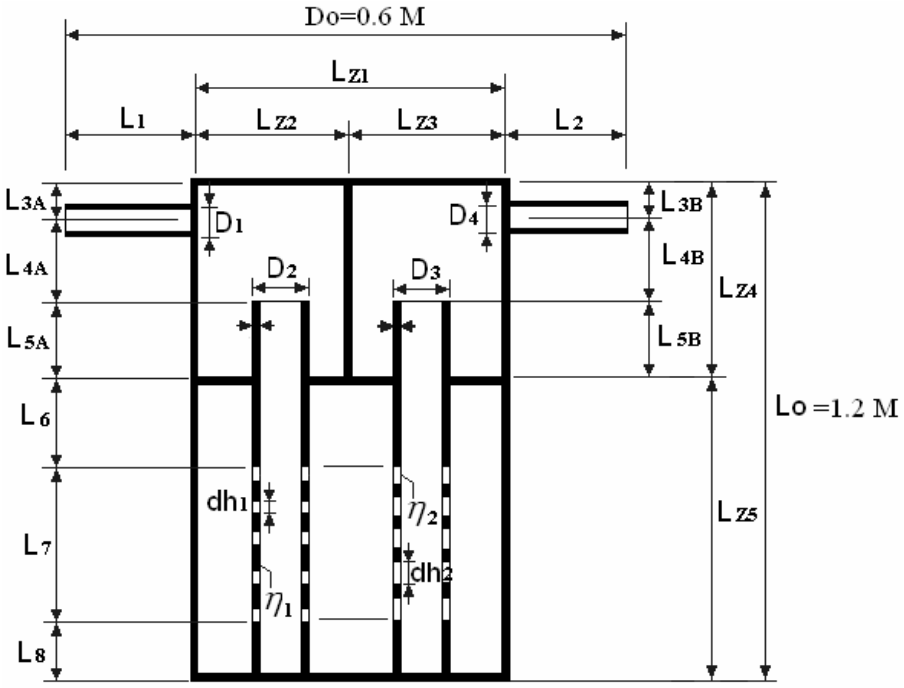

Fig. 2. The outline of a multi-chamber side inlet/outlet muffler with reverse-flow ducts.

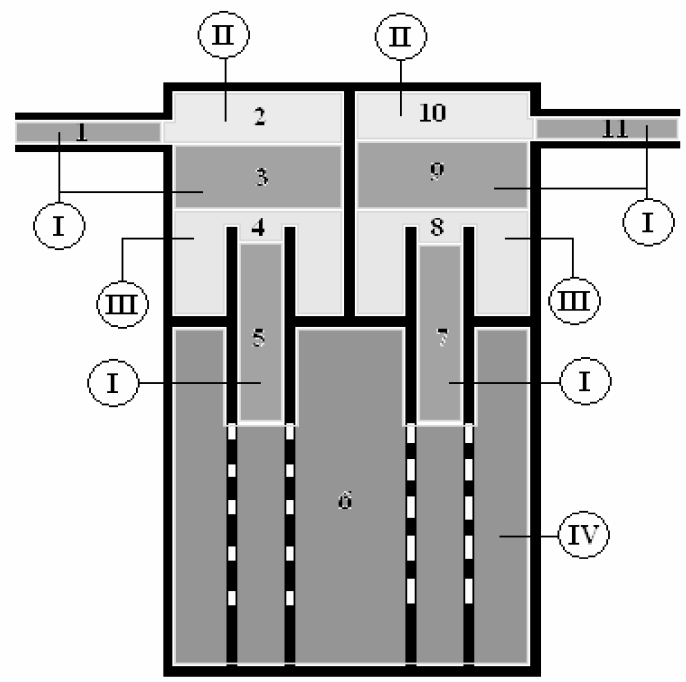

Fig. 3. A multi-chamber side inlet/outlet muffler with reverse-flow ducts.

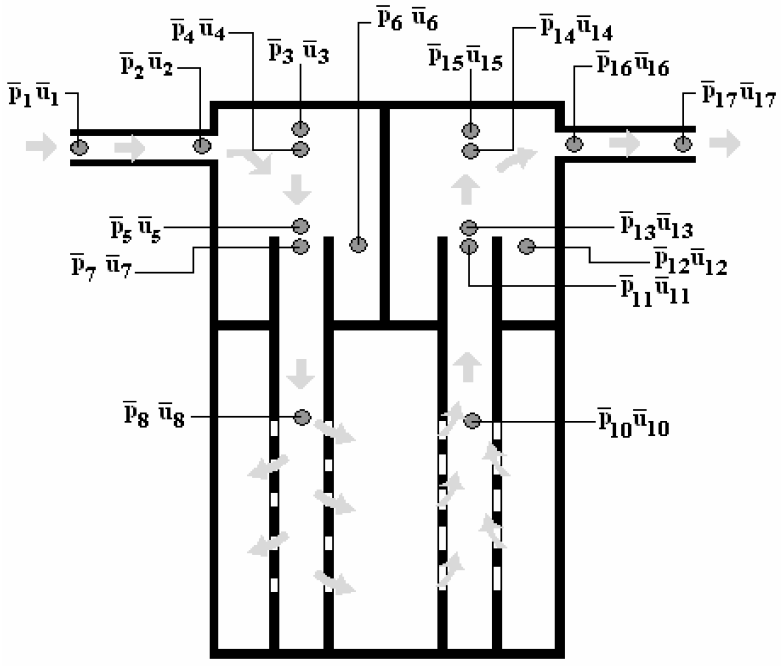

Fig. 4. Acoustical field in a multi-chamber reverse-flow perforated and side inlet/outlet muffler.

2.1. Sound transmission loss

Based on the plane wave theory deduced by MUNJAL (1987), the four-pole matrices between the adjacent two nodes are:

$$\begin{pmatrix} \overline{p}_1 \\ \rho_o c_o \overline{u}_1 \end{pmatrix} = e^{-jM_1 kL_1/(1-M_1^2)} \begin{bmatrix} TS1_{1,1} & TS1_{1,2} \\ TS1_{2,1} & TS1_{2,2} \end{bmatrix} \begin{pmatrix} \overline{p}_2 \\ \rho_o c_o \overline{u}_2 \end{pmatrix}, \tag{1}$$

$$\begin{pmatrix} \overline{p}_2 \\ \rho_o c_o \overline{u}_2 \end{pmatrix} = \begin{bmatrix} TSE1_{1,1} & TSE1_{1,2} \\ TSE1_{2,1} & TSE1_{2,2} \end{bmatrix} \begin{pmatrix} \overline{p}_4 \\ \rho_o c_o \overline{u}_4 \end{pmatrix}, \tag{2}$$

$$\begin{pmatrix} \overline{p}_4 \\ \rho_o c_o \overline{u}_4 \end{pmatrix} = e^{-jM_4 kL_{4A}/(1-M_4^2)} \begin{bmatrix} TS2_{1,1} & TS2_{1,2} \\ TS2_{2,1} & TS2_{2,2} \end{bmatrix} \begin{pmatrix} \overline{p}_5 \\ \rho_o c_o \overline{u}_5 \end{pmatrix}, \tag{3}$$

$$\begin{pmatrix} \overline{p}_5 \\ \rho_o c_o \overline{u}_5 \end{pmatrix} = \begin{bmatrix} TE1_{1,1} & TE1_{1,2} \\ TE1_{2,1} & TE1_{2,2} \end{bmatrix} \begin{pmatrix} \overline{p}_7 \\ \rho_o c_o \overline{u}_7 \end{pmatrix}, \tag{4}$$

$$\begin{pmatrix} \overline{p}_7 \\ \rho_o c_o \overline{u}_7 \end{pmatrix} = e^{-jM_7 k(L_{5A}+L_6)/(1-M_7^2)} \begin{bmatrix} TS3_{1,1} & TS3_{1,2} \\ TS3_{2,1} & TS3_{2,2} \end{bmatrix} \begin{pmatrix} \overline{p}_8 \\ \rho_o c_o \overline{u}_8 \end{pmatrix}, \tag{5}$$

$$\begin{pmatrix} \overline{p}_8 \\ \rho_o c_o \overline{u}_8 \end{pmatrix} = \begin{bmatrix} TPRF1_{1,1} & TPRF1_{1,2} \\ TPRF1_{2,1} & TPRF1_{2,2} \end{bmatrix} \begin{pmatrix} \overline{p}_{10} \\ \rho_o c_o \overline{u}_{10} \end{pmatrix}, \tag{6}$$

$$\begin{pmatrix} \overline{p}_{10} \\ \rho_o c_o \overline{u}_{10} \end{pmatrix} = e^{-jM_{10} k(L_{5B}+L_6)/(1-M_{10}^2)} \begin{bmatrix} TS4_{1,1} & TS4_{1,2} \\ TS4_{2,1} & TS4_{2,2} \end{bmatrix} \begin{pmatrix} \overline{p}_{11} \\ \rho_o c_o \overline{u}_{11} \end{pmatrix}, \tag{7}$$

$$\begin{pmatrix} \overline{p}_{11} \\ \rho_o c_o \overline{u}_{11} \end{pmatrix} = \begin{bmatrix} TE2_{1,1} & TE2_{1,2} \\ TE2_{2,1} & TE2_{2,2} \end{bmatrix} \begin{pmatrix} \overline{p}_{13} \\ \rho_o c_o \overline{u}_{13} \end{pmatrix}, \tag{8}$$

$$\begin{pmatrix} \overline{p}_{13} \\ \rho_o c_o \overline{u}_{13} \end{pmatrix} = e^{-jM_{13} kL_{4B}/(1-M_{13}^2)} \begin{bmatrix} TS5_{1,1} & TS5_{1,2} \\ TS5_{2,1} & TS5_{2,2} \end{bmatrix} \begin{pmatrix} \overline{p}_{14} \\ \rho_o c_o \overline{u}_{14} \end{pmatrix}, \tag{9}$$

$$\begin{pmatrix} \overline{p}_{14} \\ \rho_o c_o \overline{u}_{14} \end{pmatrix} = \begin{bmatrix} TSE2_{1,1} & TSE2_{1,2} \\ TSE2_{2,1} & TSE2_{2,2} \end{bmatrix} \begin{pmatrix} \overline{p}_{16} \\ \rho_o c_o \overline{u}_{16} \end{pmatrix}, \tag{10}$$

$$\begin{pmatrix} \overline{p}_{16} \\ \rho_o c_o \overline{u}_{16} \end{pmatrix} = e^{-jM_{16} kL_2/(1-M_{16}^2)} \begin{bmatrix} TS6_{1,1} & TS6_{1,2} \\ TS6_{2,1} & TS6_{2,2} \end{bmatrix} \begin{pmatrix} \overline{p}_{17} \\ \rho_o c_o \overline{u}_{17} \end{pmatrix}. \tag{11}$$

Using the matrices multiplication from Eq. (1) to Eq. (11), the system matrix between nodes 1 and 17 yields

$$\begin{pmatrix} \overline{p}_1 \\ \rho_o c_o \overline{u}_1 \end{pmatrix} = \begin{bmatrix} T_{11}^* & T_{12}^* \\ T_{21}^* & T_{22}^* \end{bmatrix} \begin{pmatrix} \overline{p}_{17} \\ \rho_o c_o \overline{u}_{17} \end{pmatrix}. \tag{12}$$

Under the assumption of a fixed thickness of the tubes ($t_1 = t_2 = 0.001$ m) and the symmetric design ($L_6 = L_8 = (L_{Z5} - L_7)/2$; $L_1 = L_2 = (D_0 - Lz_1)/2$), the sound transmission loss (STL) of a muffler is defined as (Thawani, Jayaraman, 1983)

$$STL \begin{pmatrix} Q, f, Aff_1, Aff_2, Aff_3, D_1, D_2, D_3, D_4, Aff_4, \\ Aff_5, Aff_6, Aff_7, Aff_8, dh_1, \eta_1, dh_2, \eta_2 \end{pmatrix}$$

$$= \log\left(\frac{|T_{11}^* + T_{12}^* + T_{21}^* + T_{22}^*|}{2}\right) + 10\log\left(\frac{S_1}{S_{17}}\right), \tag{13}_1$$

where

$$\begin{aligned} Aff_1 &= L_{Z1}/D_o, & Aff_2 &= L_{Z2}/L_{Z1}, \\ Aff_3 &= L_{Z4}/L_o, & Aff_4 &= L_{3A}/L_{z4}, \\ Aff_5 &= L_{3B}/L_{z4}, & Aff_6 &= L_{5A}/L_{z4}, \\ Aff_7 &= L_{5B}/L_{z4}, & Aff_8 &= L_7/L_{z5}, \\ L_0 &= L_{Z4} + L_{Z5}, & D_0 &= L_1 + L_{Z1} + L_2, \\ L_{Z1} &= L_{Z2} + L_{Z3}, & L_{Z4} &= L_{3A} + L_{4A} + L_{5A} = L_{3B} + L_{4B} + L_{5B}, \\ L_{Z5} &= L_6 + L_7 + L_8, & L_{Z1} &= L_{Z2} + L_{Z3}, \\ L_6 &= L_8 = (L_{Z5} - L_7)/2, & L_1 &= L_2 = (D_0 - Lz_1)/2. \end{aligned} \tag{13}_2$$

2.2. Overall sound power level

The silenced octave sound power level emitted from a silencer's outlet is

$$SWL_m = SWLO_m - STL_m, \tag{14}$$

where

1. $SWLO_m$ is the original SWL at the inlet of a muffler (or pipe outlet), and m is the index of the octave band frequency.
2. STL_m is the muffler's STL with respect to the relative octave band frequency.
3. SWL_m is the silenced SWL at the outlet of a muffler with respect to the relative octave band frequency.

Finally, the overall SWL_T silenced by a muffler at the outlet is

$$SWL_T = 10 \cdot \log \left\{ \sum_{m=1}^{7} 10^{SWL_m/10} \right\}$$

$$= 10 \cdot \log \left\{ \begin{array}{ll} 10^{[SWLO_m(f=63) - STL_m(f=63)]/10} + 10^{[SWLO_m(f=125) - STL_m(f=125)]/10} & \\ +10^{[SWLO_m(f=250) - STL_m(f=250)]/10} + 10^{[SWLO_m(f=500) - STL_m(f=500)]/10} & \\ +10^{[SWLO_m(f=1000) - STL_m(f=1000)]/10} + 10^{[SWLO_m(f=2000) - STL_m(f=2000)]/10} & \\ +10^{[SWLO_m(f=4000) - STL_m(f=4000)]/10} & \end{array} \right\}. \tag{15}$$

2.3. Objective function

By using the formula of Eqs. (13), (15), the objective function used in SA optimization was established.

A. STL maximization for a one-tone (f) noise

$$OBJ_1 = STL \left(\begin{array}{l} Q, f, Aff_1, Aff_2, Aff_3, D_1, D_2, D_3, D_4, Aff_4, \\ Aff_5, Aff_6, Aff_7, Aff_8, dh_1, \eta_1, dh_2, \eta_2 \end{array} \right). \tag{16}$$

B. SWL minimization for a broadband noise

To minimize the overall SWL_T, the objective function is

$$OBJ_2 = SWL_T \left(\begin{array}{l} Q, Aff_1, Aff_2, Aff_3, D_1, D_2, D_3, D_4, Aff_4, \\ Aff_5, Aff_6, Aff_7, Aff_8, dh_1, \eta_1, dh_2, \eta_2 \end{array} \right). \tag{17}$$

The related ranges of parameters are

$$\begin{aligned} f &= 500 \text{ (Hz)}, & Q &= 0.03 \text{ (m}^3\text{/s)}, \\ D_0 &= 0.6 \text{ (m)}, & L_0 &= 1.2 \text{ (m)}, \\ Aff_1 &: [0.4, 0.8], & Aff_2 &: [0.3, 0.7], \\ Aff_3 &: [0.4, 0.7], & D_1 &: [0.1, 0.3], \\ D_2 &: [0.1, 0.3], & D_3 &: [0.1, 0.3], \\ D_4 &: [0.1, 0.3], & Aff_4 &: [0.2, 0.4], \\ Aff_5 &: [0.2, 0.4], & Aff_6 &: [0.2, 0.4], \\ Aff_7 &: [0.2, 0.4], & Aff_8 &: [0.3, 0.7], \\ dh_1 &: [0.00175, 0.007], & \eta_1 &: [0.03, 0.1], \\ dh_2 &: [0.00175, 0.007], & \eta_2 &: [0.03, 0.1]. \end{aligned} \tag{18}$$

3. Simulated annealing algorithm

The simulated annealing (SA) algorithm is one kind of local search process which imitates the annealing of metal. The basic concept behind simulated annealing (SA) was first introduced and then developed by METROPOLIS *et al.* (1953) and KIRKPATRICK *et al.* (1983).

As indicated in Fig. 8, if the change in objective function (or energy) is negative (ie. $\Delta F \leq 0$), the new solution will be acknowledged as the new current solution with the transition property ($pb(X')$ of 1); if not (ie. $\Delta F > 0$), the new transition property ($pb(X')$) varied from 0–1 will be first calculated by the Boltzmann's factor ($pb(X') = \exp(-\Delta F/CT)$) as shown in Eq. (19):

$$pb(X') = \begin{cases} 1, & \Delta F \leq 0, \\ \exp\left(\dfrac{-\Delta F}{CT}\right), & \Delta F > 0, \end{cases} \tag{19}$$

$$\Delta F = OBJ(X') - OBJ(X).$$

Each successful substitution of the new current solution will lead to the decay of the current temperature by a cooling kk as

$$T_{\text{new}} = kk \cdot T_{\text{old}}. \tag{20}$$

The process is repeated until the predetermined number ($iter$) of the outer loop is reached.

4. Model check

Before performing the *SA* optimal simulation on mufflers, an accuracy check of mathematical models on three kinds of acoustical components – a one-chamber muffler with reverse-flow perforated tubes, a one-chamber muffler with extended tubes, and a one-chamber muffler with side inlet/outlet – is performed from Munjal *et al.* (1987), Chiu *et al.* (2006), and Chang *et al.* (2004) individually. As indicated in Figs. 5–7, the accuracy comparisons between the theoretical and analytical data or experimental data are in agreement. Therefore, the models of overall multi-chamber side inlet/outlet mufflers with reverse-flow and perforated tubes in conjunction with the numerical searching method are acceptable and adopted in the following optimization process.

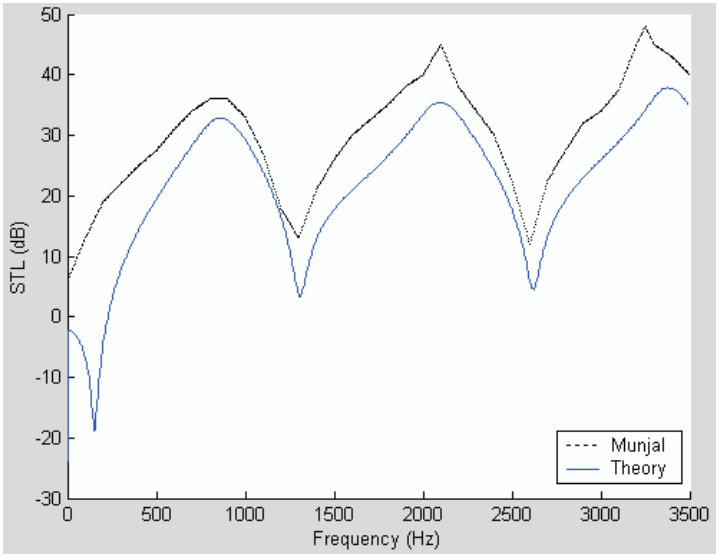

Fig. 5. Performance of a one-chamber reverse-flow perforated muffler [$D_1 = 0.0493$ (m), $D_2 = 0.0493$ (m), $D_0 = 0.1481$ (m), $L_A = L_B = 0.0064$, $L_c = 0.1286$ (m), $t_1 = t_2 = 0.0081$ (m), $dh_1 = dh_2 = 0.0035$ (m), $\eta_1 = \eta_2 = 0.039$, $M_1 = 0.1$] [analytical data is from Munjal *et al.* (1975)].

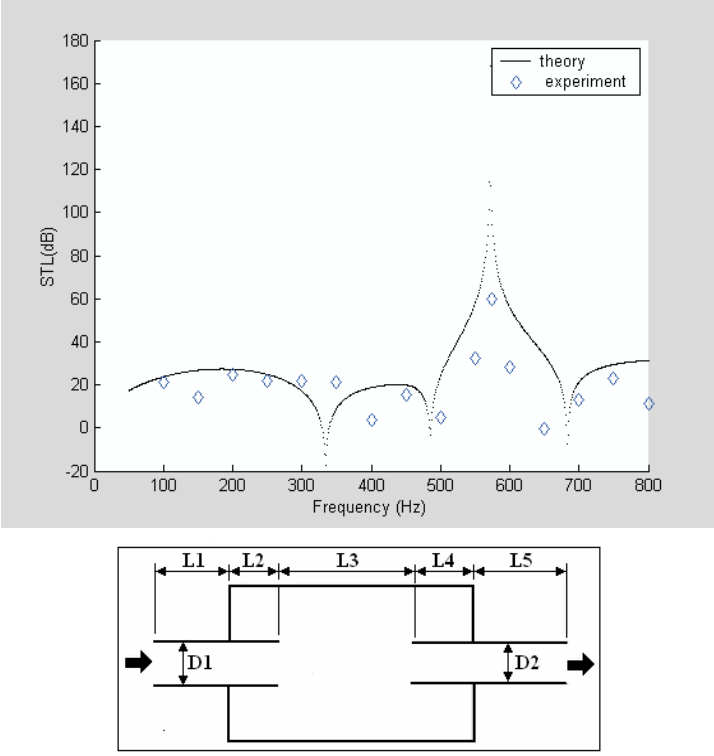

Fig. 6. Performance of a single-chamber muffler with extended tubes at the zero mean flow velocity [$D_1 = D_2 = 0.054$ (m), $L_1 = L_5 = 0.175$ (m), $L_2 = L_4 = 0.150$ (m), $L_3 = 0.504$ (m)] [experimental data is from Chiu *et al.* (2006)].

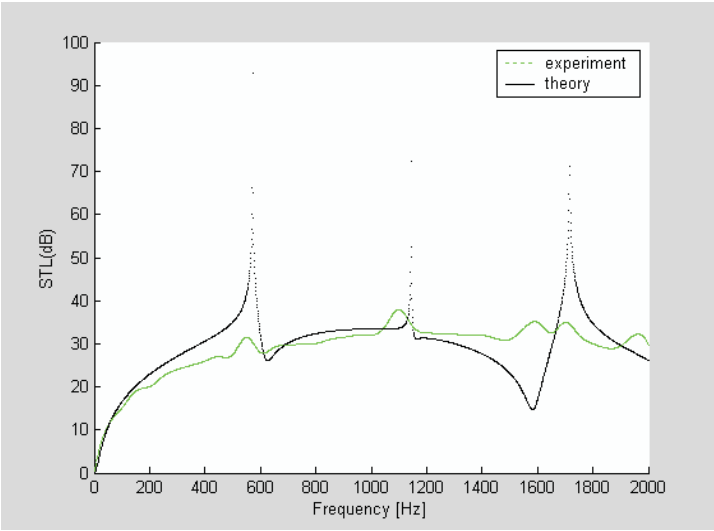

[Fig. 7]

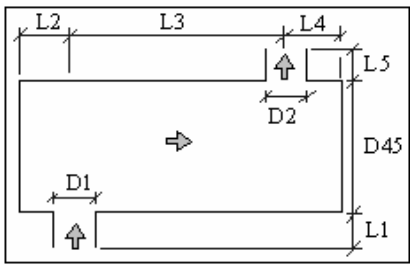

Fig. 7. Profiles of *STL* curves in theory and experiment [$D_1 = D_2 = 0.0244$ (m), $D_{45} = 0.122$ (m), $L_1 = L_5 = 0.1$ (m), $L_3 = 0.075$ (m), $L_2 = 0.15$ (m), $L_4 = 0.075$ (m)] [experimental data is from Chang *et al.* (2004)].

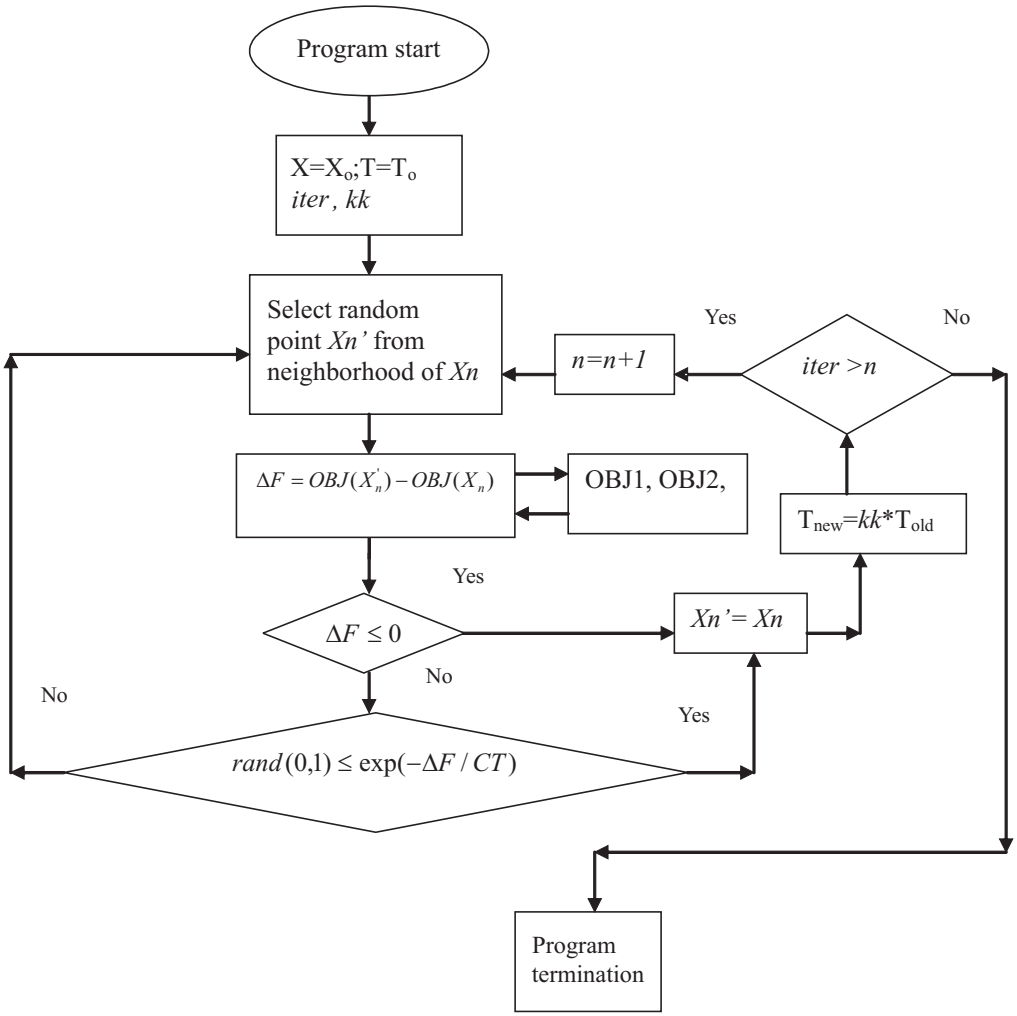

Fig. 8. Flow diagram of a *SA* optimization.

5. Case studies

In this paper, the noise reduction of a space-constrained air compressor is exemplified and shown in Fig. 1. The sound power level (SWL) inside the compressor's outlet is shown in Table 1 where the overall SWL reaches 126.8 dB. To depress the huge venting noise emitted from the compressor's outlet, a multi-chamber side inlet/outlet muffler hybridized with reverse-flow tubes is considered. To obtain the best acoustical performance within a fixed space volume, the numerical assessments linked to an SA optimizer are applied, accordingly. Before the minimization of a broadband noise is executed, a reliability check of the SA method by maximization of STL at a targeted one tone (500 Hz) has been carried out in advance. As shown in Figs. 1 and 2, the available space for a muffler is 0.6 m in width, 0.6 m in height, and 1.2 m in length. The flow rate (Q) and thickness of a perforated tube (t) are preset as 0.03 (m^3/s) and 0.001 (m), respectively; moreover, the thickness of shell made of the carbon steel is preset as 0.01 (m); the corresponding OBJ functions, space constraints, and the ranges of design parameters are summarized in Eqs. (16)–(18).

Table 1. Unsilenced SWL of an air compressor inside a duct outlet.

f (Hz)	125	250	500	1000	2000	4000
$SWLO$ (dB)	126	118	110	108	100	98

6. Results and discussion

6.1. Results

To investigate the influences of the cooling rate and the number of iterations, the ranges of the SA parameters of the cooling rate and the iterations are

$$kk = (0.90, 0.93, 0.96, 0.99); \qquad iter = (50\text{–}400).$$

The optimal results with respect to one tone and broadband noise optimizations are described as follows:

A. One-Tone Noise Optimization

By using Eqs. (16), (18), the maximization of STL at 500 Hz was performed. As indicated in Table 2, seven sets of parameters are tried. Obviously, the optimal STL can be achieved to 212.1 dB at the last set of SA parameters, at (kk, $iter$) = (0.96, 400). In addition, the related STL with respect to various cooling rates (kk) and iterations ($iter$) are plotted and illustrated in Figs. 9 and 10; moreover, the accuracy of OBJ value will be significantly improved till an iteration of 400 is reached. Consequently, it is observable that the maximal STL is precisely tuned at the targeted tone of 500 Hz.

Table 2. Optimal *STL* for a multi-chamber side inlet/outlet muffler with reverse-flow ducts (at a targeted tone of 500 Hz).

Item	*SA* parameter		Results					
	kk	*iter*						
1	2	3	4	5	6	7	8	9
1	0.90	50	Aff_1	Aff_2	Aff_3	D_1 (m)	D_2 (m)	D_3 (m)
			0.5102	0.4102	0.4827	0.1551	0.1551	0.1551
			D_4 (m)	Aff_4	Aff_5	Aff_6	Aff_7	Aff_8
			0.1551	0.2551	0.2551	0.2551	0.2551	0.4102
			η_1	dh_1 (m)	η_2	dh_2 (m)		STL (dB)
			0.003196	0.04929	0.003196	0.04929		106.4
2	0.93	50	Aff_1	Aff_2	Aff_3	D_1 (m)	D_2 (m)	D_3 (m)
			0.5793	0.4793	0.5345	0.1897	0.1897	0.1897
			D_4 (m)	$Aff4$	$Aff5$	$Aff6$	$Aff7$	$Aff8$
			0.1897	0.2897	0.2897	0.2897	0.2897	0.4793
			η_1	dh_1 (m)	η_2	dh_2 (m)		STL (dB)
			0.004104	0.06138	0.004104	0.06138		125.1
3	0.96	50	Aff_1	Aff_2	Aff_3	D_1 (m)	D_2 (m)	D_3 (m)
			0.5472	0.4472	0.5104	0.1736	0.1736	0.1736
			D_4 (m)	Aff_4	Aff_5	Aff_6	Aff_7	Aff_8
			0.1736	0.2736	0.2736	0.2736	0.2736	0.4472
			η_1	dh_1 (m)	η_2	dh_2 (m)		STL (dB)
			0.003683	0.05577	0.003683	0.05577		136.6
4	0.99	50	Aff_1	Aff_2	Aff_3	D_1 (m)	D_2 (m)	D_3 (m)
			0.6058	0.5058	0.5543	0.2029	0.2029	0.2029
			D_4 (m)	Aff_4	Aff_5	Aff_6	Aff_7	Aff_8
			0.2029	0.3029	0.3029	0.3029	0.3029	0.5058
			η_1	dh_1 (m)	η_2	dh_2 (m)		STL (dB)
			0.004451	0.06601	0.004451	0.06601		101.7
5	0.96	100	Aff_1	Aff_2	Aff_3	D_1 (m)	D_2 (m)	D_3 (m)
			0.5566	0.4566	0.5175	0.1783	0.1783	0.1783
			D_4 (m)	Aff_4	Aff_5	Aff_6	Aff_7	Aff_8
			0.1783	0.2783	0.2783	0.2783	0.2783	0.4566
			η_1	dh_1 (m)	η_2	dh_2 (m)		STL (dB)
			0.003806	0.05741	0.003806	0.05741		147.1

1	2	3	4	5	6	7	8	9
6	0.96	200	Aff_1	Aff_2	Aff_3	D_1 (m)	D_2 (m)	D_3 (m)
			0.5535	0.4535	0.5151	0.1767	0.1767	0.1767
			D_4 (m)	Aff_4	Aff_5	Aff_6	Aff_7	Aff_8
			0.1767	0.2767	0.2767	0.2767	0.2767	0.4535
			η_1	dh_1 (m)	η_2	dh_2 (m)		STL (dB)
			0.003765	0.05686	0.003765	0.05686		161.8
7	0.96	**400**	Aff_1	Aff_2	Aff_3	D_1 (m)	D_2 (m)	D_3 (m)
			0.5516	**0.4516**	**0.5137**	**0.1758**	**0.1758**	**0.1758**
			D_4 (m)	Aff_4	Aff_5	Aff_6	Aff_7	Aff_8
			0.1758	**0.2758**	**0.2758**	**0.2758**	**0.2758**	**0.4516**
			η_1	dh_1 (m)	η_2	dh_2 (m)		STL (dB)
			0.003740	**0.05653**	**0.003740**	**0.05653**		**212.1**

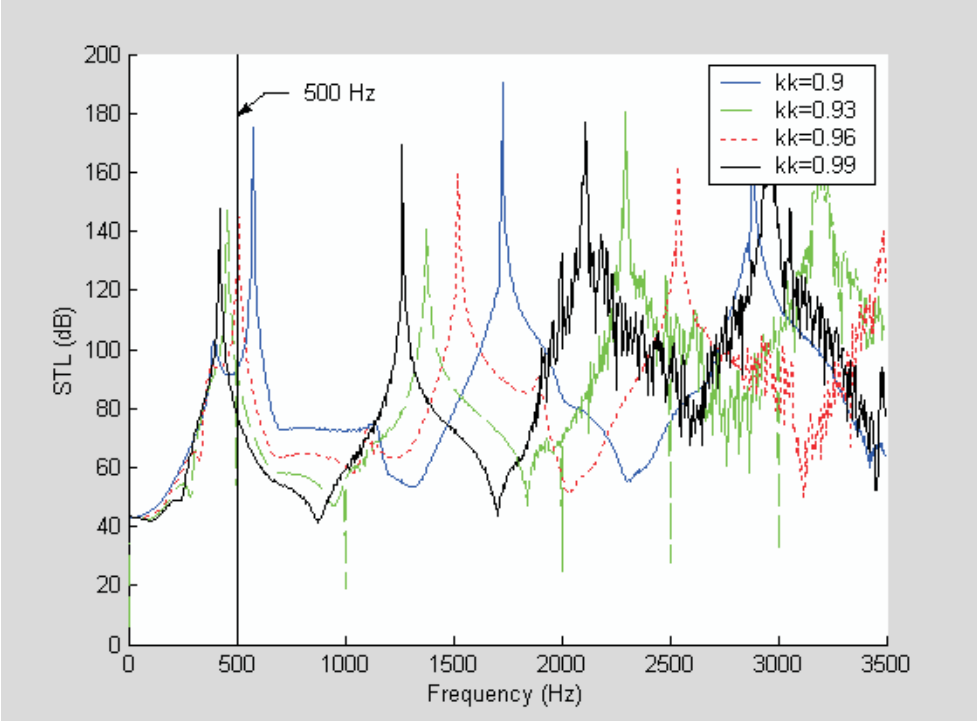

Fig. 9. *STL* curves with respect to frequencies at various cooling rates for a multi-chamber reverse-flow and inlet/outlet side muffler [$iter = 50$, targeted tone = 500 Hz].

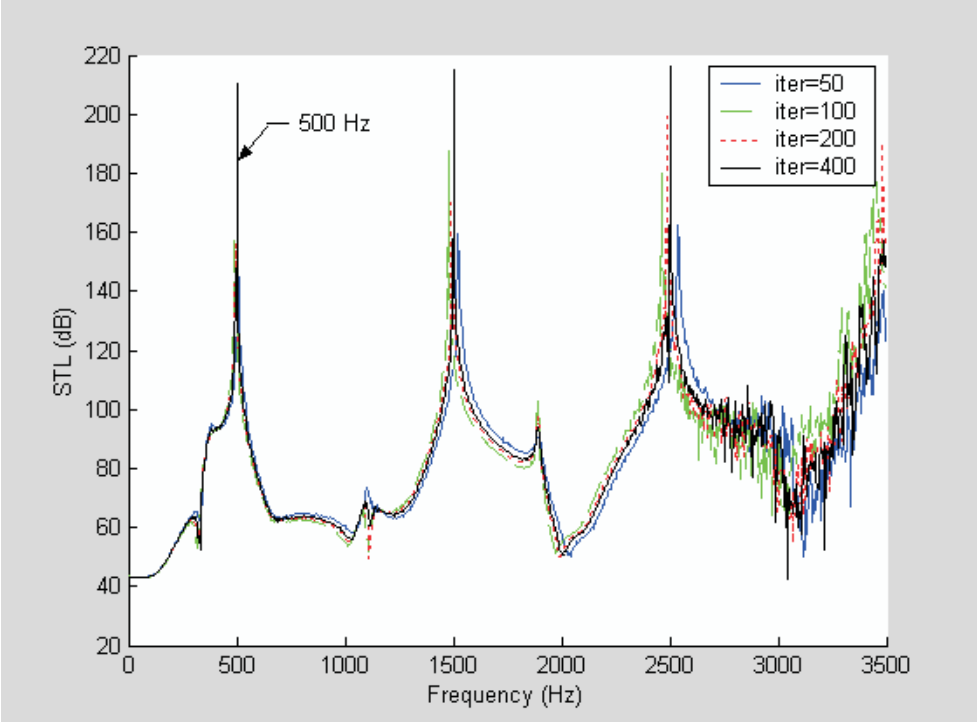

Fig. 10. *STL* curves with respect to frequencies at various iterations for a multi-chamber reverse-flow and inlet/outlet side muffler [$kk = 0.96$, targeted tone = 500 Hz].

B. Broadband Noise Optimization

By using Eqs. (17), (18), the optimal design parameters in minimizing the compressor's sound power level are achieved and summarized in Table 3.

Table 3. Optimal *STL* for a multi-chamber side inlet/outlet muffler with reverse-flow ducts (for a broadband noise).

Item	*SA* parameter		Results					
	kk	*iter*						
1	2	3	4	5	6	7	8	9
1	0.90	50	Aff_1	Aff_2	Aff_3	D_1 (m)	D_2 (m)	D_3 (m)
			0.6007	0.5007	0.5506	0.2004	0.2004	0.2004
			D_4 (m)	Aff_4	Aff_5	Aff_6	Aff_7	Aff_8
			0.2004	0.3004	0.3004	0.3004	0.3004	0.5007
			η_1	dh_1 (m)	η_2	dh_2 (m)		SWL_T (dB)
			0.004385	0.06513	0.004385	0.06513		70.09

1	2	3	4	5	6	7	8	9
2	0.93	50	Aff_1	Aff_2	Aff_3	D_1 (m)	D_2 (m)	D_3 (m)
			0.6100	0.5100	0.5575	0.2050	0.2050	0.2050
			D_4 (m)	Aff_4	Aff_5	Aff_6	Aff_7	Aff_8
			0.2050	0.3050	0.3050	0.3050	0.3050	0.5100
			η_1	dh_1 (m)	η_2	dh_2 (m)		SWL_T (dB)
			0.004506	0.06674	0.004506	0.06674		69.05
3	0.96	50	Aff_1	Aff_2	Aff_3	D_1 (m)	D_2 (m)	D_3 (m)
			0.7027	0.6027	0.6270	0.2513	0.2513	0.2513
			D_4 (m)	Aff_4	Aff_5	Aff_6	Aff_7	Aff_8
			0.2513	0.3513	0.3513	0.3513	0.3513	0.6027
			η_1	dh_1 (m)	η_2	dh_2 (m)		SWL_T (dB)
			0.005723	0.08297	0.005723	0.08297		62.54
4	0.99	50	Aff_1	Aff_2	Aff_3	D_1 (m)	D_2 (m)	D_3 (m)
			0.6429	0.5429	0.5822	0.2214	0.2214	0.2214
			D_4 (m)	Aff_4	Aff_5	Aff_6	Aff_7	Aff_8
			0.2214	0.3214	0.3214	0.3214	0.3214	0.5429
			η_1	dh_1 (m)	η_2	dh_2 (m)		SWL_T (dB)
			0.004938	0.07251	0.004938	0.07251		66.09
5	0.96	100	Aff_1	Aff_2	Aff_3	D_1 (m)	D_2 (m)	D_3 (m)
			0.7182	0.6182	0.6387	0.2591	0.2591	0.2591
			D_4 (m)	Aff_4	Aff_5	Aff_6	Aff_7	Aff_8
			0.2591	0.3591	0.3591	0.3591	0.3591	0.6182
			η_1	dh_1 (m)	η_2	dh_2 (m)		SWL_T (dB)
			0.005926	0.08569	0.005926	0.08569		62.22
6	0.96	**200**	Aff_1	Aff_2	Aff_3	D_1 (m)	D_2 (m)	D_3 (m)
			0.7159	**0.6159**	**0.6369**	**0.2579**	**0.2579**	**0.2579**
			D_4 (m)	Aff_4	Aff_5	Aff_6	Aff_7	Aff_8
			0.2579	**0.3579**	**0.3579**	**0.3579**	**0.3579**	**0.6159**
			η_1	dh_1 (m)	η_2	dh_2 (m)		SWL_T (dB)
			0.005896	**0.08528**	**0.005896**	**0.08528**		**53.64**

In Table 3, the optimal design data occurred in the sixth set. The related STL with respect to various cooling rates (kk) and iterations ($iter$) are plotted and illustrated in Figs. 11 and 12. As a result, the original SWL can be dramatically reduced from 126.8 dB to 53.6 dB.

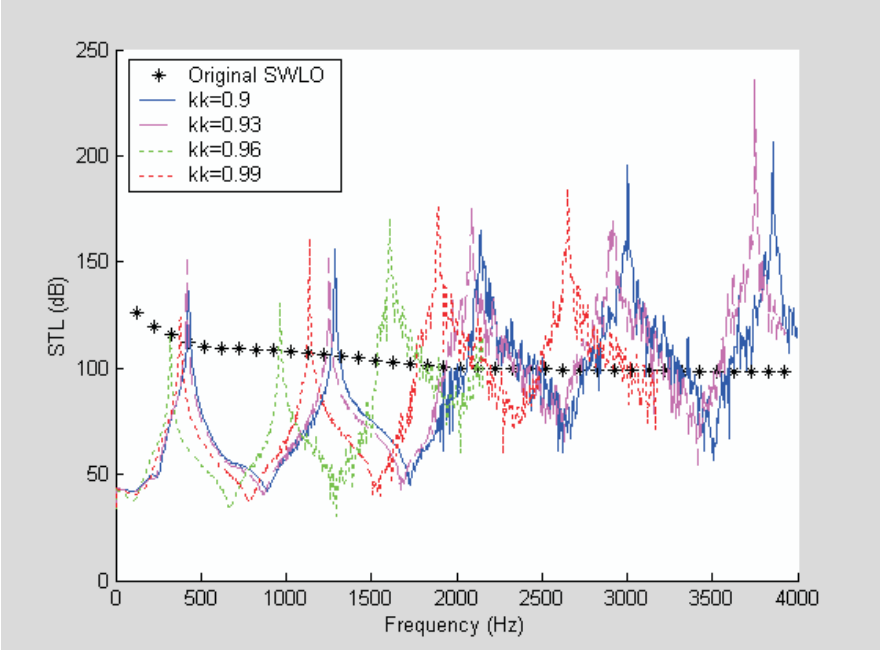

Fig. 11. *STL* curves with respect to frequencies at various cooling rates (kk) for a multi-chamber side inlet/outlet muffler with reverse-flow ducts [$iter = 50$; for a broadband noise].

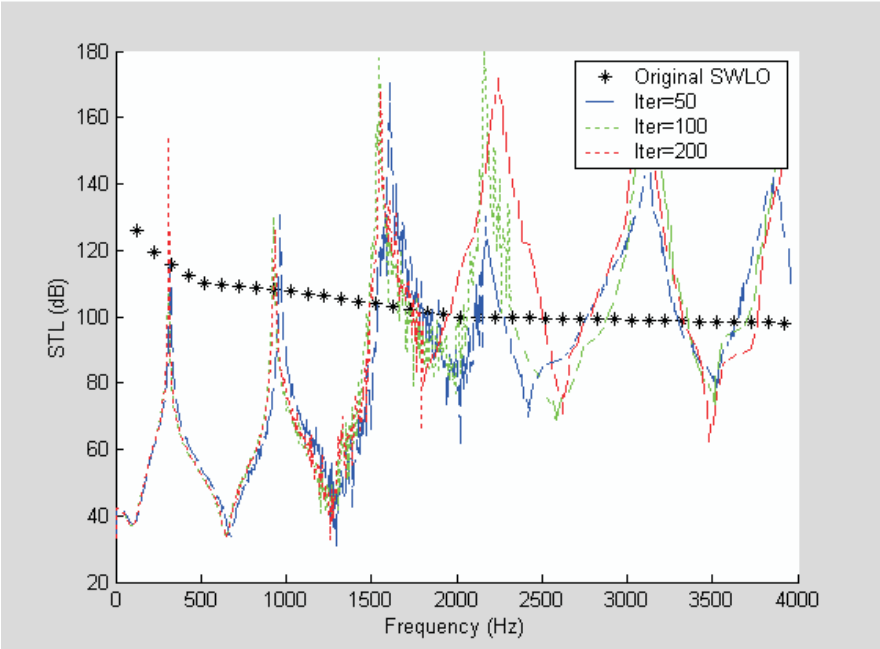

Fig. 12. *STL* curves with respect to frequencies at various iterations ($iter$) for a multi-chamber side inlet/outlet muffler with reverse-flow ducts [$kk = 0.96$; for a broadband noise].

6.2. Discussion

For a pure tone's optimization discussed in Subsec. 6.1 and shown in Figs. 9, 10, the maximal *STL* has been precisely tuned at the targeted pure tone of 500 Hz. As a result of the above observation, the *SA* method, therefore, is reliably used in the muffler's shape optimization.

In dealing with a broadband noise in which the spectrum is complicated and emitted from a noisy compressor, the selection of appropriate *SA* parameter sets is essential in searching for a better shape design solution during the optimization process. As illustrated in Table 3, the optimal design data has been achieved at (*kk, iter*) of (0.96, 200). Moreover, the largest noise reduction of 73.2 dB can be reached.

Consequently, considering the noise emission and the resonances from the shell, an amendment by adding a cladding with one layer of sound-absorbing material is suggested.

7. Conclusion

It has been shown that two kinds of *SA* parameters – *kk, iter* – play essential roles in seeking a better solution during the *SA* optimization. A higher iteration will lead to a set of enhanced shape design data. Before the broadband noise optimization is performed, the pure-tone optimization of a muffler has been carried out. Results reveal that the maximal *STL* is precisely tuned at the targeted tone of 500 Hz; therefore the *SA* method used in the muffler's shape optimization is reliable.

As investigated in Subsec. 6.1, in order to efficiently reduce a broadband noise emitted from a noisy compressor in which the spectrum is complicated, searching of an appropriate *STL* profile by adjusting the muffler's dimensions (Aff_1, Aff_2, Aff_3, D_1, D_2, D_3, D_4, Aff_4, Aff_5, Aff_6, Aff_7, Aff_8, dh_1, η_1, dh_2, η_2) via the *SA* optimizer is required. As indicated in Figs. 11 and 12, the optimized *STL* curves will be shifted to reduce the overall *SWL* by varying the *SA* parameter – *kk*. Besides, the acoustical performance will be improved when the iteration (*iter*) is increased from 50 to 200. The simulated results reveal that the original *SWL* can be dramatically reduced from 126.8 dB to 53.6 dB. Therefore, a multi-chamber side inlet/outlet muffler with reverse-flow ducts exhibiting an excellent acoustical ability can be considered for a noisy and space-constrained venting system. Moreover, considering the noise emission and the resonances from the shell, an extra cladding adhered onto the muffler's shell will be necessary when dealing with a tremendous noise source. Consequently, the use of the *SA* optimization in the multi-chamber side inlet/outlet muffler with reverse-flow ducts' shape design is indeed easier and more efficient when compared to the trial calculations.

Acknowledgment

The authors acknowledge the financial support of the National Science Council (NSC 97-2622-E-235-002-CC3), ROC.

References

1. Alley B.C., Dufresne R.M., Kanji N., Reesal M.R. (1989), *Costs of workers' compensation claims for hearing loss*, Journal of Occupational Medicine, **31**, 134–138.
2. Chang Y.C., Yeh L.J., Chiu M.C. (2004), *Numerical studies on constrained venting system with side inlet/outlet mufflers by GA optimization*, Acta Acustica united with Acustica, **1**, 1, 1–11.
3. Chang Y.C., Yeh L.J., Chiu M.C. (2005), *Shape optimization on double-chamber mufflers using Genetic Algorithm*, Proc. ImechE Part C: Journal of Mechanical Engineering Science, **10**, 31–42.
4. Chiu M.C. (2009), *SA Optimization on multi-chamber mufflers hybridized with perforated plug-inlet under space constraints*, Archives of Acoustics, **34**, 3, 305–343.
5. Chiu M.C., Yeh L.J., Chang C.Y., Lai G.J., Her M.G., Lan T.S. (2006), *Shape optimization of single-chamber mufflers with side inlet/outlet by using the boundary element method, mathematic gradient method and genetic algorithm*, Proceedings of the 23th National Conference of the Chinese Society of Mechanical Engineers, R.O.C.
6. Davis D.D, Stokes J.M., Moorse L. (1954), *Theoretical and experimental investigation of mufflers with components on engine muffler design*, NACA Report, 1192.
7. Kirkpatrick S., Gelatt C.D., Vecchi M.P. (1983), *Optimization by simulated annealing*, Science, **220**, 4598, 671–680.
8. Magrab E.B. (1975), *Environmental Noise Control*, John Wiley and Sons, New York.
9. Metropolis A., Rosenbluth W., Rosenbluth M.N., Teller H., Teller E. (1953), *Equation of static calculations by fast computing machines*, J. Chem. Phys., **21**, 6, 1087–1092.
10. Munjal M.L. (1987), *Acoustics of Ducts and Mufflers with Application to Exhaust and Ventilation System Design*, John Wiley and Sons, New York.
11. Munjal M.L, Rao K.N., Sahasrabudhe A.D. (1987), *Aeroacoustic analysis of perforated muffler components*, Journal of Sound and Vibration, **114**, 2, 173–188.
12. Peat K.S. (1988), *A numerical decoupling analysis of perforated pipe silencer elements*, Journal of Sound and Vibration, **123**, 2, 199–212.
13. Sullivan J.W., Crocker M.J. (1978), *Analysis of concentric tube resonators having unpartitioned cavities*, Acous. Soc. Am., **64**, 207–215.
14. Sullivan J.W. (1979), *A method of modeling perforated tube muffler components I: theory*, Acous. Soc. Am., **66**, 772–778.
15. Sullivan J.W., *A method of modeling perforated tube muffler components II: theory*, Acous. Soc. Am., **66**, 779–788.

16. Thawani P.T., Jayaraman K. (1983), *Modeling and applications of straight-through resonators*, Acous. Soc. Am., **73**, 4, 1387–1389.

17. Yeh L.J., Chang Y.C., Chiu M.C. (2006), *Numerical studies on constrained venting system with reactive mufflers by GA optimization*, International Journal for Numerical Methods in Engineering, **65**, 1165–1185.

18. Yeh L.J., Chang Y.C., Chiu M.C., Lai G.J. (2003), *Computer-aided optimal design of a single-chamber muffler with side inlet/outlet under space constraints*, Journal of Marine Science and Technology, **11**, 4, 1–8.